CANCER INNOVATION

ORIGINAL ARTICLE

MAPK4 facilitates angiogenesis by inhibiting the ERK pathway in non-small cell lung cancer

Jing Chen[1,2] | Jing Yang[1,2] | Yufang Liu[1,2] | Xu Zhao[1,2] | Juanjuan Zhao[1,2] |
Lin Tang[1,2] | Mengmeng Guo[1,2] | Ya Zhou[1,3] | Chao Chen[1,2] |
Dongmei Li[1,2] | Zhenke Wen[4] | Guiyou Liang[5] | Lin Xu[1,2] (iD)

[1]Special Key Laboratory of Gene Detection & Therapy of Guizhou Province, Zunyi, Guizhou, China

[2]Department of Immunology, Zunyi Medical University, Zunyi, Guizhou, China

[3]Department of Medical Physics, Zunyi Medical University, Zunyi, Guizhou, China

[4]Institute of Biomedical, Soochow University, Suzhou, Jiangsu, China

[5]Department of Cardiovascular Surgery, Affiliated Hospital of Guizhou Medical University, Guiyang, Guizhou, China

Correspondence
Lin Xu, Department of Immunology, Zunyi Medical University, Zunyi 563003, Guizhou, China.
Email: xulinzhouya@163.com and xulinzhouya@zmu.edu.cn

Guiyou Liang, Department of Cardiovascular Surgery, Affiliated Hospital of Guizhou Medical University, Guiyang 550004, Guizhou, China.
Email: liangguiyou@gmc.edu.cn

Abstract

Background: Angiogenesis plays an important role in the occurrence and development of non-small cell lung cancer (NSCLC). The atypical mitogen-activated protein kinase 4 (MAPK4) has been shown to be involved in the pathogenesis of various diseases. However, the potential role of MAPK4 in the tumor angiogenesis of NSCLC remains unclear.

Methods: Adult male C57BL/6 wild-type mice were randomly divided into the control group and p-siMAPK4 intervention group, respectively. The cell proliferation was analyzed with flow cytometry and immunofluorescence staining. The vascular density in tumor mass was analyzed by immunofluorescence staining. The expressions of MAPK4 and related signaling molecules were detected by western blot analysis and immunofluorescence staining, and so on.

Results: We found that the expression of MAPK4, which was dominantly expressed in local endothelial cells (ECs), was correlated with tumor angiogenesis of NSCLC. Furthermore, MAPK4 silencing inhibited the proliferation and migration abilities of human umbilical vein ECs (HUVECs).

Abbreviations: AKT, protein kinase B; ECs, endothelial cells; ERK1/2, extracellular regulated protein kinases 1/2; FCM, flow cytometry; HUVECs, human umbilical vein endothelial cells; JNK, c-Jun n-terminal kinase; Ki67, cell proliferation nuclear antigen; LLC, Lewis lung carcinoma; MAPK4, mitogen-activated protein kinase 4; MEK, mitogen-activated extracellular signal-regulated kinase; NF-κB, nuclear factor κB; NSCLC, non-small cell lung cancer; p21, cyclin-dependent kinase inhibitor 1A; p-AKT, phosphorylated AKT; p-ERK1/2, phosphorylated ERK1/2; p-JNK, phosphorylated JNK; p-MEK, phosphorylated MEK; p-NF-κB, phosphorylated NF-κB; Raf, rapidly accelerated fibrosarcoma; Ras, rat sarcoma; RNAi, RNA interference; siRNA, small interfering RNA; WT, wild-type.

Jing Chen, Jing Yang, and Yufang Liu contributed equally to this work.

Global gene analysis showed that MAPK4 silencing altered the expression of multiple genes related to cell cycle and angiogenesis pathways, and that MAPK4 silencing increased transduction of the extracellular regulated protein kinases 1/2 (ERK1/2) pathway but not Akt and c-Jun n-terminal kinase pathways. Further analysis showed that MAPK4 silencing inhibited the proliferation and migration abilities of HUVECs cultured in tumor cell supernatant, which was accompanied with increased transduction of the ERK1/2 pathway. Clinical data analysis suggested that the higher expression of MAPK4 and CD34 were associated with poor prognosis of patients with NSCLC. Targeted silencing of MAPK4 in ECs using small interfering RNA driven by the CD34 promoter effectively inhibited tumor angiogenesis and growth of NSCLC in vivo.

Conclusion: Our results reveal that MAPK4 plays an important role in the angiogenesis and development of NSCLC. MAPK4 may thus represent a new target for NSCLC.

KEYWORDS

angiogenesis, endothelial cell, MAPK4, NSCLC, p-ERK1/2

1 | INTRODUCTION

Non-small cell lung cancer (NSCLC) is a highly morbid and lethal disease with a poor prognosis that accounts for 85% of all lung cancers [1, 2]. Approximately 70% of patients with newly diagnosed NSCLC are over 65 years of age and more than half have metastatic or locally advanced NSCLC [3]. Despite recent advances in the diagnosis and treatment of NSCLC, the 5-year overall survival rate remains low [4], especially in the elderly population. The low survival rate is in part because of the complex etiology of NSCLC tumorigenesis. Research has shown that angiogenesis plays an important role in the occurrence and development of NSCLC. Angiogenesis is necessary for tumor cells to further grow after penetrating the epithelial basement membrane and has important clinical significance for tumor growth and metastasis and even prognosis [5, 6]. For example, Zhang et al. [7] found that high expression of ubiquitin-specific protease 22 enhanced angiogenesis and recurrence of NSCLC. Zhuo et al. [8] found that cadherin-2 induced angiogenesis, thus promoting the metastasis of lung adenocarcinoma. The growth and migration of endothelial cells (ECs) are the key factors in mediating neovascularization [9, 10]. Therefore, angiogenesis inhibitors, such as bevacizumab, ramucirumab, and nintedanib, have been proposed as clinical antitumor drugs [11, 12]. Although antiangiogenic therapies have been extensively evaluated in patients with NSCLC, these antiangiogenic agents have showed no significant positive effects on all stages of NSCLC. Therefore, it is of great significance to further study the antiangiogenesis mechanisms in NSCLC, especially the molecular mechanism underlying the growth and migration of ECs. Additionally, the combination of antiangiogenic agents with other therapies, such as gene therapy [13] and traditional Chinese medicine [14], should be investigated, as these combinations may have a better clinical therapeutic effect than any single therapeutic agent [15, 16].

Mitogen-activated protein kinase 4 (MAPK4; also called ERK4 or p63MAPK), a 578 aa protein with a molecular weight of ~70 kDa, is a member of the atypical MAPK family [17]. Accumulating evidence has shown that MAPK4 is an important intrinsic regulatory factor in the development of various organs and diseases. For example, our recent work showed that MAPK4 is involved in the pathological changes of acute lung injury (ALI) [18] and autoimmune hepatitis [19]. Recent studies also demonstrated that MAPK4 is also closely related to the development of multiple cancers [20–22]. For example, MAPK4 has been reported to modulate the immune response in cancers and mediate tumorigenesis in cancers such as cervical cancer [23], ovarian cancer [24], gastric cancer [25], and breast cancer [26]. Moreover, MAPK4 was shown to promote the growth of human NSCLC cell lines [27], indicating that it might play an important role in the occurrence and development of NSCLC. Therefore, it is of significance to explore the potential role of MAPK4 in angiogenesis in tumors, including NSCLC, which

would be much valuable for the development of new clinical strategies against tumors.

In the present study, we assessed the potential role of MAPK4 in angiogenesis of NSCLC using a murine NSCLC tumor model. Our data showed that the expression of MAPK4 was dominant in ECs of tumor tissue, accompanied by an increase in local angiogenesis of NSCLC. MAPK4 silencing inhibited the proliferation and migration abilities of human umbilical vein ECs (HUVECs), accompanied with increased transactivation of extracellular regulated protein kinases 1/2 (ERK1/2) pathway. Analysis of clinical data indicated that the high expression of both MAPK4 and CD34 in tumor tissues were associated with poor prognosis of patients with NSCLC. Finally, targeted intervention of MAPK4 expression in ECs not only affected angiogenesis but also markedly inhibited the growth of NSCLC in vivo. Collectively, our findings reveal a previously unknown role of MAPK4 in the angiogenesis of NSCLC and indicate that targeted intervention of the expression of MAPK4 in ECs may be a viable clinical antiangiogenic therapeutic strategy for NSCLC treatment.

2 | MATERIALS AND METHODS

2.1 | Animals

C57BL/6 wild-type (WT) mice (5–6 weeks old) provided by Zunyi Medical University Laboratory Animal Care were housed under specific pathogen-free conditions at Zunyi Medical University. All animal experiments were performed following the Guidelines for the Care and Use of Laboratory Animals (Ministry of Health, China, 1998). The experimental procedures were approved by the ethical guidelines of the Zunyi Medical University Laboratory Animal Care and Use Committee (permit number 2018016).

2.2 | Cell culture

Lewis lung carcinoma (LLC) cells were cultured in high-glucose Dulbecco's modified Eagle medium containing 10% fetal bovine serum at 37°C in 5% CO_2. HUVECs and A549 cells were cultured in RPMI 1640 medium containing 10% fetal bovine serum at 37°C in 5% CO_2. HUVECs (Cellosaurus accession ID: CVCL_CVCL_B7UI) and A549 (CVCL_0023) cells were purchased from the Conservation Genetics CAS Kunming Cell Bank (KCB200603YJ) and short tandem repeat-profiled at the Conservation Genetics CAS Kunming Cell Bank. All experiments were performed with mycoplasma-free cells.

2.3 | Establishment of the NSCLC model

Adult male C57BL/6 mice were randomly divided into the control group and p-siMAPK4 intervention group, respectively. To establish the mouse NSCLC tumor model, the mice were implanted with the LLC NSCLC cell line (5×10^5 tumor cells/mouse).

2.4 | Immunofluorescence

Frozen sections of tumor tissues were obtained and sliced into 6-μm-thick sections. After deparaffinization and rehydration, the slides were incubated with the corresponding primary antibodies (anti-MAPK4: Proteintech, 26102-1-AP; anti-phosphorylated ERK1/2 [p-ERK1/2]: Abcam, ab201015; anti-CD34: Abcam, ab8158; anti-cell proliferation nuclear antigen [Ki67; Abcam, 92742]) and secondary antibodies (Alexa Fluor 647: Cell Signaling, 4414S; Alexa Fluor 488: Abcam, ab150077; anti-MAPK6: Absin, abs133606; anti-NLK: Abcam, ab26050; anti-MAPK15: Thermo Fisher, PA5-105740). The slides were then counterstained with 4′,6-diamidino-2-phenylindole (Beyotime, C1002) and observed under an Olympus microscope.

2.5 | RNA extraction, reverse transcription, and quantitative real-time polymerase chain reaction (PCR)

Total RNA was isolated from HUVECs using RNAiso Plus (TAKARA, 9108) following the manufacturer's instructions. RNA was quantified and reverse transcribed to complementary DNA (cDNA) with the PrimeScript 1st Strand cDNA Synthesis kit SuperMix for qPCR (TAKARA, 6110A) and following the manufacturer's instructions. Real-time PCR amplifications were performed on the Bio-Rad CFX96 detection system (Bio-Rad Laboratories) in 20 μL reaction volumes containing cDNA, primers, and TB Green® Premix Ex Taq™ II (Tli RNaseH Plus) (TAKARA, RR820A). The relative expression levels of genes were calculated by the comparative threshold cycle method with glyceraldehyde 3-phosphate dehydrogenas (GAPDH) messenger RNA (mRNA) as the internal reference.

2.6 | Flow cytometry (FCM)

The expression of Ki-67 (Ki67-Alexa Fluor®488 antibodies, 350507, BioLegend) and the cell cycle distribution of cells were detected by FCM with a Beckman Gallios

flow cytometer (Beckman Coulter, Inc.). Intracellular staining was conducted following the manufacturer's manual (eBioscience, Fixation/Permeabilization kit, 00-5123-43).

2.7 | Western blot analysis

HUVECs were homogenized in ice-cold lysis buffer (Key-GEN BioTECH, KGP2100) following the manufacturer's instructions. Equal amounts of protein were separated by 10% sodium dodecyl-sulfate polyacrylamide gel electrophoresis and transferred onto polyvinylidene difluoride membranes. Membranes were incubated with 5% skim milk in phosphate-buffered saline (PBS) for 1 h. Immunoblotting was performed using monoclonal antibodies against cyclin-dependent kinase inhibitor 1A (p21) (Proteintech, 10355-1-AP), Cyclin A (Abcam, ab185619), Cyclin B1 (Abcam, ab181593), MAPK4 (Proteintech, 26102-1-AP), protein kinase B (AKT) (Abcam, ab8805), phosphorylated AKT (p-AKT) (Abcam, ab38449), ERK1/2 (Abcam, ab184699), p-ERK1/2 (Abcam, ab201015), nuclear factor κB (NF-κB) (Abcam, ab32536), phosphorylated NF-κB (p-NF-κB) (Abcam, 97726), c-Jun n-terminal kinase (JNK) (Abcam, ab179461), phosphorylated JNK (p-JNK) (Abcam, ab124956), rat sarcoma (Ras) (Abcam, ab52939), rapidly accelerated fibrosarcoma (Raf) (Abcam, ab137435), p-Raf (Abcam, ab173539), mitogen-activated extracellular signal-regulated kinase (MEK) (Abcam, ab178876), phosphorylated MEK (p-MEK) (Abcam, ab194754), and GAPDH (Abcam, 181602). Membranes were washed in PBS with Tween 20 and subsequently incubated with horseradish peroxidase-conjugated anti-rabbit secondary antibody (Abcam, 7074S). Signals were detected and analyzed using a Bio-Rad ChemiDoc MP Imaging System (Bio-Rad Laboratories). GAPDH was used as the internal reference.

2.8 | Plasmid construction

A series of CD34 promoter truncations (UCSC, ENSMUST00000016638.7) and the MAPK4 small interfering RNA (siRNA) construct were synthesized and cloned into the pGL3.0 basic vector between the SacI and XhoI sites (Gene Create, GS1-1905109). The vectors were purified using an EndoFree Plasmid Maxi Kit (12123) and used for experiments after verification by DNA sequencing.

2.9 | Plasmid transfection in vivo

Plasmid (75 μg) and Entranster™-in vivo (Engreen, 18668-11-2) (150 μL) were mixed at a ratio of 1:2 used to form the in vivo transfection complex. After incubation at room temperature for 15 min, the transfection complex (containing 75 μg plasmid) was injected into the distal portion of the tumor once every 2 days for a total of three times.

2.10 | Hematoxylin-eosin (H&E) staining

Tumor and lung tissues from the mouse xenograft tumor model were subjected to paraffin embedding, sectioning, and HE staining with the assistance of the Department of Pathology, Affiliated Hospital of Zunyi Medical University.

2.11 | siRNA tranfection

HUVECs were inoculated into 24-well plates and cultured in RPMI 1640 medium containing 10% fetal bovine serum at 37°C in 5% CO_2. When cells reached 70%–80% confluence, the cells were transfected with MAPK4 siRNA (50 nM) using Lipofectamine 3000 reagent (Invitrogen, L3000015) following the manufacturer's instructions.

2.12 | Cell counting kit-8 (CCK-8) assay

CCK-8 reagent (MCE, HY-K0301) in fresh complete medium (1: 9) was added to transfected HUVECs seeded in 96-well plates and incubated for 2 h. The optical density at 450 nm (OD_{450}) in each well was measured in the dark with a microplate reader, and the absorbance curve was generated.

2.13 | Colony formation assay

Transfected HUVECs were seeded in six-well plates at 50 or 100 cells per well for different experimental setting, respectively. After 14 days of culture, 4% paraformaldehyde was added for 15 min and 0.5% crystal violet staining solution was then added for 20 min. The plates were washed and the colonies were counted and photographed.

2.14 | Tube formation assay

Matrigel basement membrane matrix (BD, 356234) was used to coat 96-well plates (60 μL per well). After the Matrigel solidified, HUVECs were seeded into the wells (2×10^4 cells per well) and cultured in serum-free complete medium for 12 h. Tube formation was observed under a microscope (Olympus IX-51 inverted optical microscope).

2.15 | Patients and tissue samples

Lung cancer paraffin samples were obtained from Shanghai Outdo Biotech Company (HlugA180Su03). This study was approved by the Ethics Committee of the Shanghai Outdo Biotech Company.

2.16 | Statistical analysis

Statistical analysis was performed using GraphPad Prism 8 software (GraphPad Prism 8.0.1). One-way analysis of variance followed by Bonferroni's post hoc test was applied for multiple comparisons, and Student's t test was used when two conditions were compared. A two-tailed $p < 0.05$ was considered statistically significant. All data are shown as the mean $\pm$ SEM values. Survival was evaluated by the Kaplan–Meier method.

3 | RESULTS

3.1 | MAPK4 expression and angiogenesis of NSCLC

To explore the potential relationship between MAPK4 and angiogenesis during the development of NSCLC, we examined the expression of atypical MAPK family members at indicated time points after establishment of the NSCLC tumor model in WT mice (Figure 1a). The tumor volume and weight markedly increased over time in the NSCLC model mice (Figure 1b,c) Furthermore, the expression level of CD34, a marker of ECs, in tumor tissues increased, indicating the increase of local vascular density during the tumorigenesis of NSCLC (Figure 1d). Further analysis showed that the expression level of MAPK4 was elevated in CD34$^+$ ECs in tumor tissues (Figure 1e,f), but no changes were observed for the other atypical MAPK family members, such as MAPK6, NLK, and MAPK15 (Supporting Information S1: Figure S1A–D). These results indicated a positive correlation between MAPK4 and vascular density during the progression of NSCLC. We further found that MAPK4 and CD34 strongly colocalized in tumors (Figure 1g,h). Together, these data showed that MAPK4 is abundantly expressed in ECs of NSCLC and its expression is directly proportional to tumor angiogenesis.

3.2 | MAPK4 silencing inhibits the proliferation of ECs in vitro

Our results showed that MAPK4 was highly expressed in ECs in NSCLC tumors. We thus next explored whether MAPK4 contributes to angiogenesis in NSCLC. Because of the limitation of obtaining primary ECs in tumors, we used HUVECs. We then examined MAPK4 function using transiently transfected MAPK4 RNA interference (RNAi). Quantitative real-time PCR, western blot analysis, and immunofluorescence results showed that the expression of MAPK4 in MAPK4 RNAi-transfected HUVECs was markedly lower than that in the control group (Figure 2a–c). CCK-8 assay results indicated that the proliferation ability of MAPK4 RNAi-transfected HUVECs was markedly decreased (Figure 2d) in a time-dependent manner (Figure 2e). Moreover, the colony-forming and tube-forming abilities of MAPK4 RNAi-transfected cells were decreased (Figure 2f,g). Notably, scratch assay results showed that the migration ability of MAPK4 RNAi-transfected cells was unchanged compared with the control group (Supporting Information S1: Figure S2A–E).

We further examined the influence of MAPK4 on cell cycle distribution. FCM results showed that the percentage of G0/G1-phase cells in the MAPK4 RNAi-transfected group was markedly lower than that in the control group, whereas the percentage of S-phase cells was increased (Figure 2h), indicating that MAPK4 silencing induces S phase arrest. We next examined the expressions of cell cycle-related proteins. Real-time PCR results showed that the mRNA levels of cyclin-dependent kinases (CDKs) were lower in the MAPK4 RNAi-transfected group than in the control group (Figure 2i). Western blot analysis results showed that cyclin A and p21 expressions in the MAPK4 RNAi-transfected group were lower than those in the control group (Figure 2j), but the level of cyclin B1 was not significantly different (Figure 2j). These results suggested that MAPK4 silencing inhibited cell proliferation and induced S phase arrest of ECs.

3.3 | MAPK4 silencing inhibits the growth of HUVECs by regulating the Raf/MEK/ERK1/2 signaling pathway

To further investigate the role and mechanism of MAPK4 in angiogenesis, we used global gene expression analysis to evaluate gene expression changes after MAPK4 silencing. RNA sequencing revealed that 542 genes were upregulated and 608 genes were downregulated in the MAPK4 RNAi-transfected group (Figure 3a). Gene Ontology analysis showed that MAPK-related genes were significantly upregulated (Figure 3b). In line with in vitro experiments, cell cycle-related genes and DNA replication-related genes were significantly downregulated in the MAPK4 RNAi-transfected group (Figure 3c). These data suggested that MAPK4 silencing influences pathways involved in proliferation and the cell cycle in ECs.
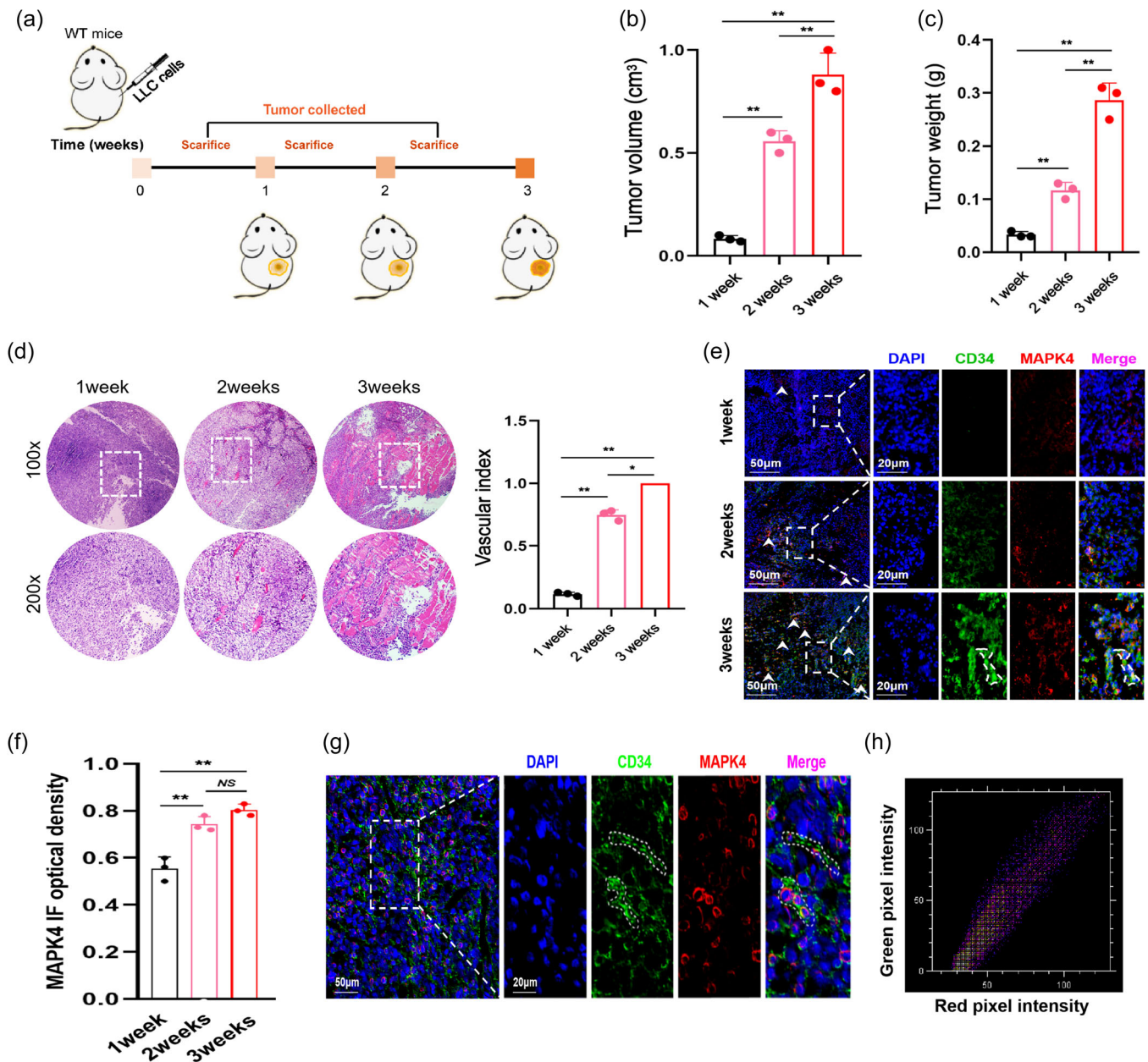
FIGURE 1 Mitogen-activated protein kinase 4 (MAPK4) expression during the development of non-small cell lung cancer (NSCLC). (a) Schematic diagram showing subcutaneous injection of Lewis lung carcinoma (LLC) cells (5×10^5) into the right flanks of wild-type (WT) mice. (b) Tumor volume. (c) Tumor weight. (d) Tumor pathology was analyzed by hematoxylin-eosin (H&E) staining. (e) The expression levels of MAPK4 in tumors was analyzed by immunofluorescence and (f) quantified. (g) The colocalization of CD34 and MAPK4 in tumors were analyzed by immunofluorescence. (h) Colocation coefficient between CD34 and MAPK4 expression were quantified by ImageJ. Representative data from three independent experiments were shown. *$p < 0.05$, **$p < 0.01$. NS, no significance.

Our above data showed that MAPK4 silencing inhibited the growth of ECs and influences multiple intracellular signaling pathways including other MAPKs pathways. We thus further examined potential changes in these signaling pathways. Western blot analysis results showed that ERK1/2, AKT, p-AKT, NF-κB, p-NF-κB, JNK, and p-JNK levels were not significantly different in the MAPK4 siRNA-transfected and control groups

(Figure 3d,e). However, p-ERK1/2 was markedly increased in the MAPK4 siRNA-transfected group (Figure 3e). Therefore, we speculated that MAPK4 silencing may lead to activation of ERK1/2, but not AKT, JNK, and NF-κB signaling pathways in ECs.

To further examine changes in the ERK1/2 pathway, a three-kinase module, we used western blot analysis to evaluate MEK (MAPKK) and Raf (MAPKKK), and their
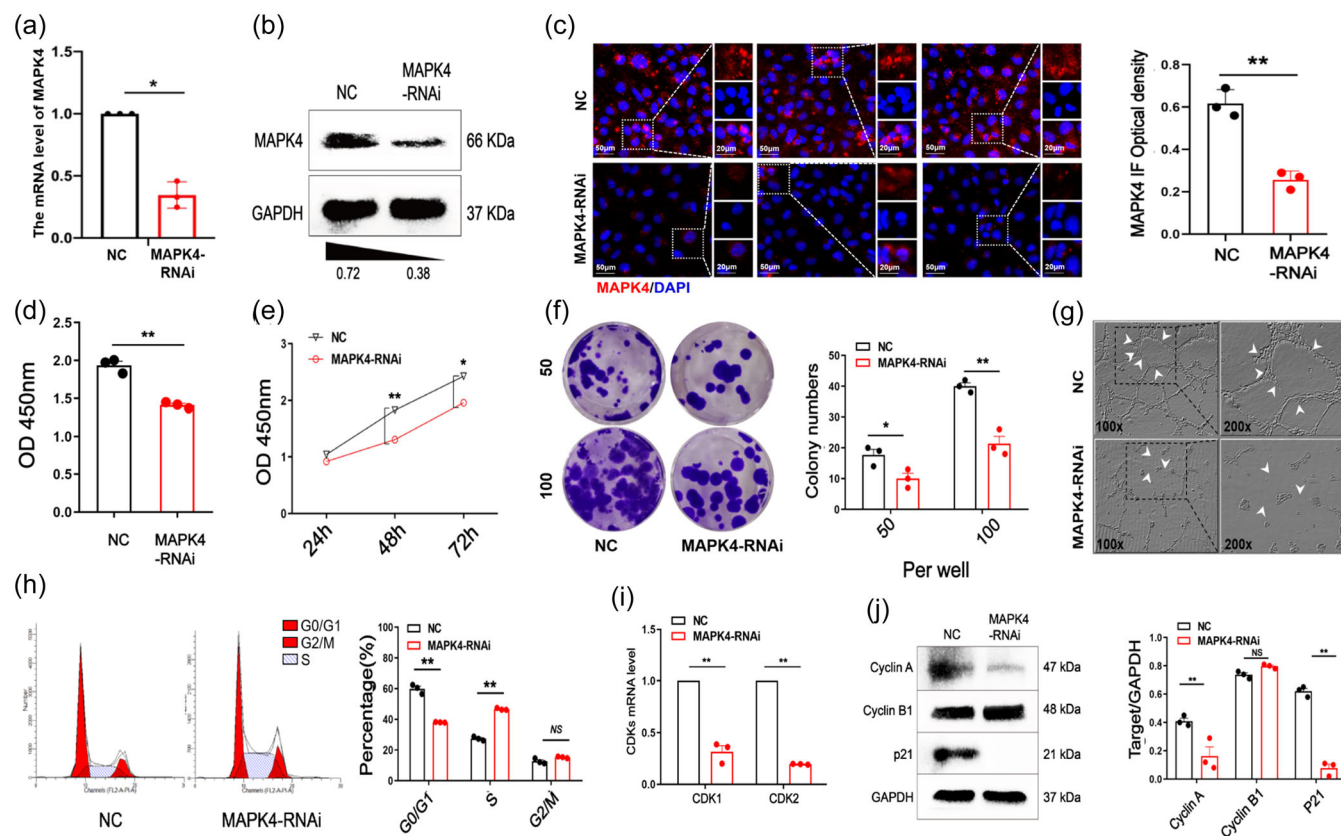
FIGURE 2 Mitogen-activated protein kinase 4 (MAPK4) silencing inhibits the proliferarion of endothelial cells (ECs) in vitro. Human umbilical vein ECs (HUVECs) were transiently transfected with MAPK4 small interfering RNA (siRNA) (50 nM) in 24-well plates via Lipofectamine 3000 reagent in vitro, 48 h later. (a) The expression of MAPK4 was analyzed by real-time polymerase chain reaction (PCR). (b) Western blot analysis and (c) immunofluorescence staining were used to detect and quantitatively analyze MAPK4 expression in the two groups. (d, e) Cell counting kit-8 (CCK-8) assay was used to evaluate the proliferation of HUVECs 24, 48, and 72 h after transfection of MAPK4-RNA interference (RNAi). (f) Colony formation assay was used to evaluate the colony-forming ability of HUVECs and the colonies were counted. (g) The tube-forming ability of HUVECs was evaluated by tube formation assay. (h) The cell cycle distribution was evaluated by fluorescence-activated cell sorting. (i) The expression levels of CDKs in HUVECs were determined by real-time PCR. (j) Western blot analysis was used to evaluate the expression of Cyclin A, Cyclin B1, and cyclin-dependent kinase inhibitor 1A (p21) in HUVECs. Representative data from three independent experiments were shown. $*p < 0.05$, $**p < 0.01$. NS, no significance.

phosphorylated forms. The levels of p-MEK, Raf, and p-Raf in the MAPK4 siRNA-transfected group were markedly increased compared with levels in the control group (Figure 3f). To further confirm the effect of MAPK silencing on the ERK1/2 pathway, we used immuno-fluorescence to examine activation of the ERK1/2 pathway in MAPK4 RNAi-transfected HUVECs in vitro by immunofluorescence. The results confirmed that p-ERK1/2 expression in the MAPK4 RNAi-transfected group was increased compared with controls (Figure 3g,h).

To reproduce the tumor microenvironment in vivo, we cultured HUVECs in the supernatant of human NSCLC A549 cells and examined changes of growth in HUVECs after MAPK4 silencing. Immunofluorescence results confirmed that MAPK4 expression was significantly lower in

the MAPK4 RNAi-transfected group compared with the control group (Figure 4a). Consistent with the above data, cell counting, CCK-8 assay, tube formation assay, and FCM results showed that the proliferation and tube-forming abilities of HUVECs were decreased in the MAPK4 RNAi-transfected group (Figure 4b–e). Similar results were obtained in HUVECs cultured in the supernatant of A549 cells. The expressions of p-Raf, p-MEK, and p-ERK1/2 were increased in the MAPK4 RNAi-transfected group, while ERK1/2, MEK, Raf, and Ras levels were not significantly different (Figure 4f,g). We further examined p-ERK1/2 expression by immunofluorescence and obtained similar results (Figure 4h,i). Together, these data indicated that the effects of MAPK4 silencing in the growth of HUVECs are related to changes in the transduction of the Raf/MEK/ERK1/2 pathway.
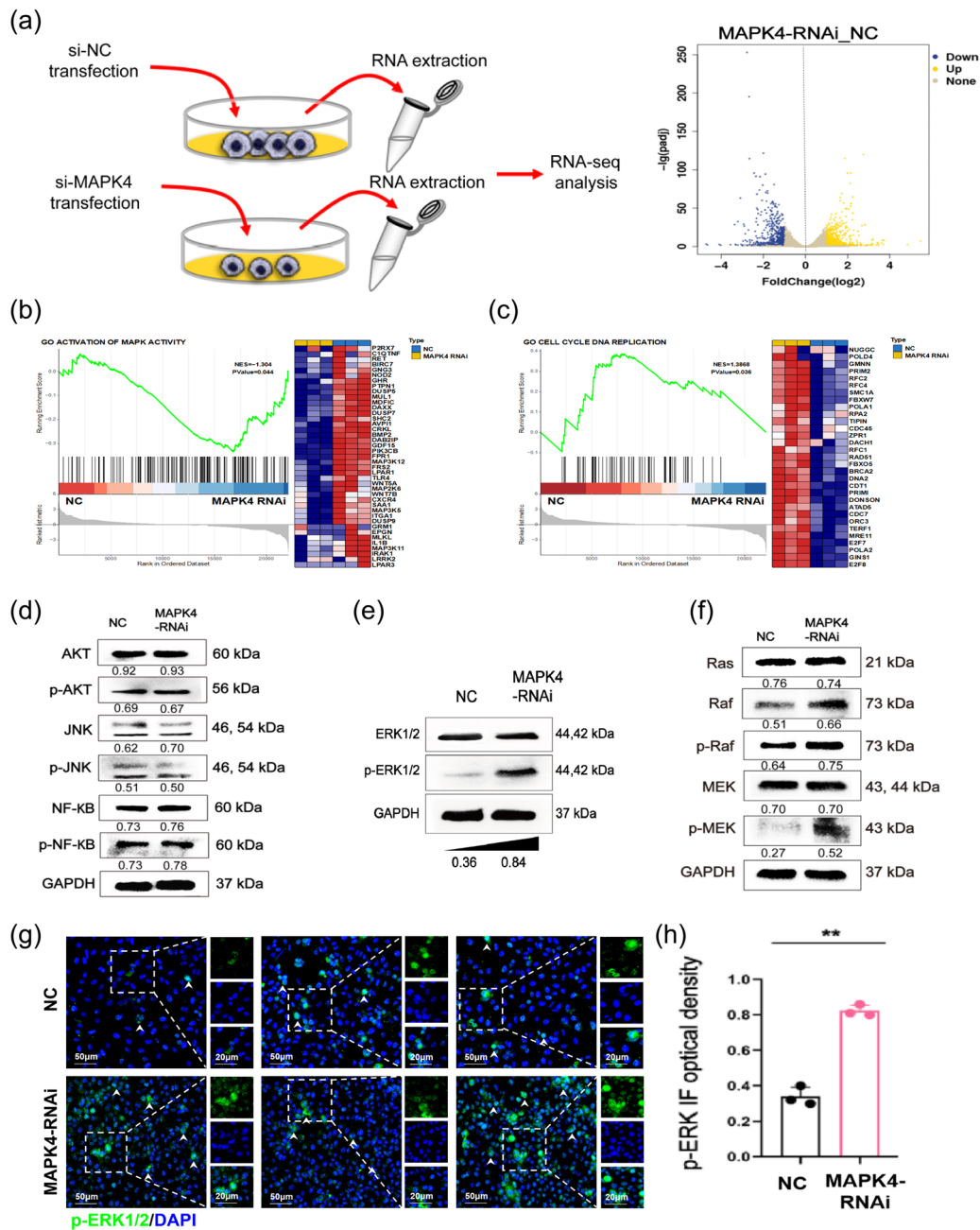
FIGURE 3 Mitogen-activated protein kinase 4 (MAPK4) silencing inhibits the proliferation of endothelial cells (ECs) by regulating the Raf/MEK/ERK1/2 signaling pathway. Human umbilical vein ECs (HUVECs) were transiently transfected with MAPK4 small interfering RNA (siRNA) (50 nM) in 24-well plates via Lipofectamine 3000 reagent in vitro. (a) Volcano plot showing genes with differential expression in MAPK4-silenced HUVECs (MAPK4 HUVECs) compared with NC HUVECs, as determined by RNA sequencing (RNA-seq). $n = 3$ per group. (b, c) Gene set enrichment analysis plots (left) and heat maps (right) of the RNA-seq data for NC HUVECs and MAPK4 HUVECs. (d) Western blot analysis was used to evaluate the levels of protein kinase B (AKT), phosphorylated AKT (p-AKT), c-Jun n-terminal kinase (JNK), phosphorylated JNK (p-JNK), nuclear factor κB (NF-κB), phosphorylated NF-κB (p-NF-κB), (e) ERK1/2, phosphorylated ERK1/2 (p-ERK1/2), (f) rat sarcoma (Ras), Raf, p-Raf, MEK, and phosphorylated MEK (p-MEK) in HUVECs. (g) 24 h after transfection, transfected cells were treated with the p-ERK1/2 inhibitor and cultured for another 24 h. (h) Immunofluorescence was used to evaluate and quantitatively analyze the p-ERK1/2 level in HUVECs. Representative data from three independent experiments are shown. **$p < 0.01$. ERK1/2, extracellular regulated protein kinases 1/2; MEK, mitogen-activated extracellular signal-regulated kinase; Raf, rapidly accelerated fibrosarcoma.

3.4 | High expression of MAPK4/CD34 is associated with poor survival of patients with NSCLC

We found that MAPK4 promotes the growth of NSCLC by regulating tumor angiogenesis. To verify the relationship between MAPK4 and angiogenesis in clinical samples, we performed tissue microarray-based immunofluorescence analysis of MAPK4 expression and examined the relationship between MAPK4 and CD34 in NSCLC samples (Figure 5a). In line with previous work [19], our results showed that MAPK4 expression in

cancer tissues was markedly higher than that in adjacent tissues (Figure 5b). However, there was no correlation between MAPK4 expression and sex, age, or other clinical characteristics (Table 1). Moreover, the expression level of MAPK4 in CD34-positive ECs in cancer tissues was significantly higher than that in adjacent tissues (Figure 5c). Furthermore, patients with NSCLC with high MAPK4/CD34 showed a shorter survival rate (Figure 5d). These results suggested that MAPK4 is highly expressed in cancer tissues of patients with NSCLC and, the prognosis of patients with NSCLC with MAPK4^{high}/CD34^{high} tumors is poor.
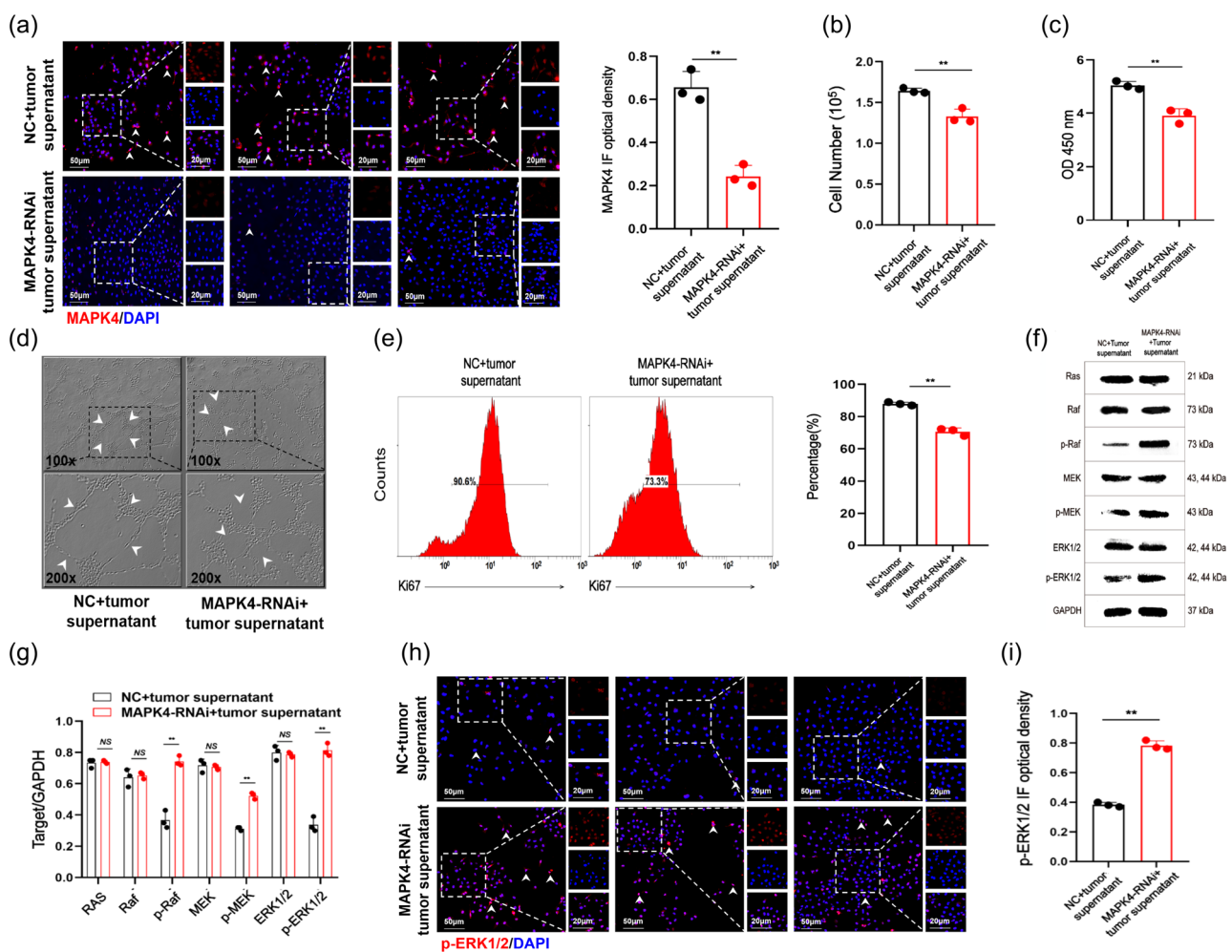

FIGURE 4 Mitogen-activated protein kinase 4 (MAPK4) silencing inhibits endothelial cell (EC) growth. Human umbilical vein ECs (HUVECs) were cultured in the supernatant of human non-small cell lung cancer (NSCLC) cells and transiently transfected with MAPK4 small interfering RNA (siRNA) (50 nM) in 24-well plates via Lipofectamine 3000 reagent in vitro. (a) The expression of MAPK4 in HUVECs was detected by immunofluorescence. (b) The number of cells was determined by cell counting. (c) Cell counting kit-8 (CCK-8) assay was used to evaluate the proliferation ability of HUVECs. (d) The tube-forming ability of HUVECs was evaluated by tube formation assay. (e) The expression of ki-67 in HUVECS was detected by fluorescence-activated cell sorting. (f, g) Extracellular regulated protein kinases 1/2 (ERK1/2) and phosphorylated ERK1/2 (p-ERK1/2) in HUVECs was detected by western blot analysis. (h, i) The expression of p-ERK1/2 in HUVECs was detected by immunofluorescence analysis and calculated. Representative data from three independent experiments are shown. **$p < 0.01$, NS, no significance.
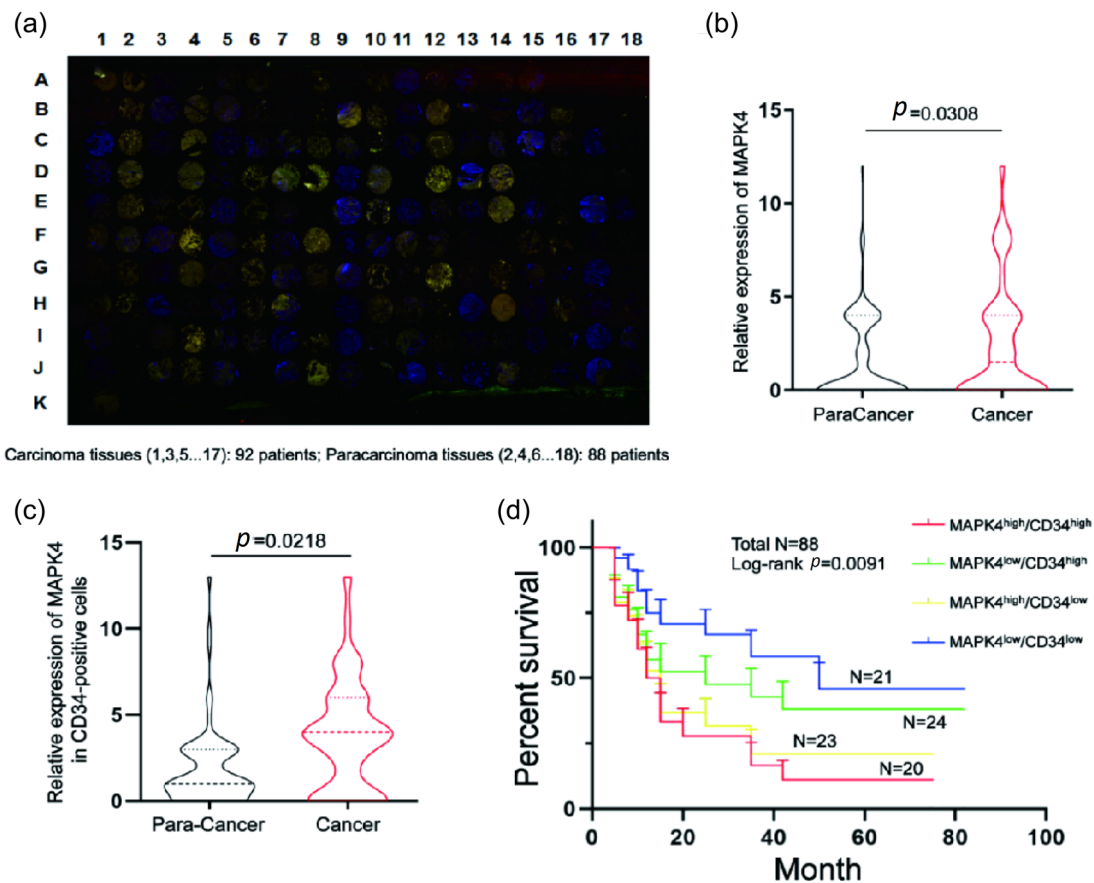
FIGURE 5 The expression of mitogen-activated protein kinase 4 (MAPK4) in the tumor tissue of patients with clinical non-small cell lung cancer (NSCLC). (a) The microarray of NSCLC tissues obtained from relevant patients was analyzed by multiplex immunofluorescence staining of CD34 and MAPK4. MAPK4 staining is shown in red, CD34 staining is shown in green, and 4′,6-diamidino-2-phenylindole (DAPI) staining is shown in blue. Carcinoma tissues (1, 3, 5...17): 92 samples; paracarcinoma tissues (2, 4, 6...18): 88 samples. (b) The expression of MAPK4 in carcinoma and paracarcinoma clinical samples from patients with NSCLC were analyzed, and the H-scores were calculated. (c) Comparison of MAPK4 expression in CD34-positive cells between cancer and adjacent tissues. (d) The 5-year overall survival rate in the four groups was determined through Kaplan–Meier analysis.

3.5 | Targeted silencing of MAPK4 in ECs inhibits the growth of NSCLC in vivo

As the expression of MAPK4 was proportional to tumor angiogenesis and MAPK4 silencing inhibited the growth and migration ability of ECs, we then further investigated the potential value of MAPK4 as an antiangiogenesis target in NSCLC. The data showed that the tumor growth was slower in the p-siMAPK4 intervention group (Figure 6a). Additionally, tumor volumes were markedly smaller, and tumor weights were markedly lower in the p-siMAPK4 intervention group (Figure 6b–d). H&E staining revealed that local vascular density of tumors in the p-siMAPK4 group was decreased (Figure 6e). The levels of CD34$^+$ ECs in tumors were also reduced (Figure 6f,g). Notably, MAPK4 expression was markedly decreased in CD34$^+$ ECs but not in NSCLC cells (Figure 6f,h). Furthermore, Ki67 expression in tumors

was lower in the p-siMAPK4 intervention group (Figure 6i,j). Therefore, these data suggested that targeted silencing of MAPK4 in ECs effectively inhibited local angiogenesis and subsequently reduced the growth of NSCLC.

Next, we observed the distributions of p-siMAPK4 plasmids in several organs and tissues to evaluate the potential influence of MAPK4-targeting interventions in the body. The data showed that p-siMAPK4 was dominantly enriched in vascularized tissues, such as lung, heart, and tumor tissues (Supporting Information S1: Figure S3A). However, MAPK4 expression was markedly downregulated in tumor tissues compared with other tissues (Supporting Information S1: Figure S3B). We also observed no significant changes in histology and weight in six organs and tissues, including heart, liver, spleen, lung, brain, and colon, between the groups (Supporting Information S1: Figures S3C–H and S4A). To confirm

TABLE 1 Correlations of MAPK4 expression with clinical characteristics of patients with NSCLC.

Characteristics	Total	MAPK4 in cancer		χ^2	p
		Low	High		
Age (years)					
≥60	55	25	30	1.212	0.271
<60	33	19	14		
Sex					
Male	49	22	27	1.151	0.283
Female	39	22	17		
Histological grade					
I/II	56	28	28	0.000	1.000
III	32	16	16		
T					
T1–2	57	26	31	0.281	0.596
T3–4	19	10	9		
N					
N0	34	14	20	0.720	0.396
N1–3	33	17	16		
Tumor size					
≥5	19	10	9	0.281	0.596
<5	57	26	31		
Clinical stage					
I–II	39	17	22	0.433	0.511
III–IV	25	13	12		
ALK					
Negative	72	35	37	0.446	0.307
Positive	9	6	3		
EGFR					
Negative	67	31	36	1.564	0.211
Positive	21	13	8		

Abbreviations: ALK, anaplastic lymphoma kinase; CDK, cyclin-dependent kinase; EGFR, epidermal growth factor receptor; MAPK4, mitogen-activated protein kinase 4; NSCLC, non-small cell lung cancer.

these findings, we examined the concentration of serum AST, ALT, and other key indicators for these organs and tissues. The results showed that these biochemistry indicators were not significantly changed between the groups (Supporting Information S1: Figure S4B–G). Together, these data suggested that MAPK4 may be a potential antiangiogenic target for NSCLC, and CD34 promoter-operated siMAPK4 may be a valuable strategy for clinical intervention.

4 | DISCUSSION

Our current study reveals that MAPK4 was abundantly expressed in ECs and its high expression positively correlated with tumor angiogenesis. MAPK4 silencing inhibited the proliferation and migration abilities of HUVECs in vitro. Mechanistically, MAPK4 silencing inhibited the proliferation and migration abilities of HUVECs by affecting the ERK1/2 pathway, accompanied by changes in the expression of multiple genes associated with cell cycle and angiogenesis. Notably, the expression of MAPK4 in CD34-positive cells was closely related with poor prognosis in patients with clinical NSCLC. Finally, targeted silencing of MAPK4 in ECs using siRNA driven by the CD34 promoter effectively inhibited the angiogenesis and growth of NSCLC in vivo.

The MAPK family is a family of serine/threonine kinases that play a central role in transducing extra-cellular signals to induce various reactions within the cells [28]. The MAPK family is divided into two categories: typical MAPKs and atypical MAPKs. Typical MAPKs include ERK1/2, JNK 1/2/3, p38 isoforms (α, β, γ, and δ), and ERK5 [29]. Atypical MAPKs include MAPK4, MAPK6, MAPK15, and NLK [17]. Accumulating evidence has supported an association between MAPKs, including MAPK4, and various types of malignant tumors, including prostate cancer [30], ovarian cancer [24], and NSCLC [31, 32]. MAPK4 promotes prostate cancer by concerted activation of androgen receptors and AKT [30]. miR-127-3p inhibits the proliferation of rat ovarian cancer cells by downregulating MAPK4 [24], and the overexpression of MAPK4 promotes the growth of NSCLC cell lines by activating the AKT/mTOR signaling pathway [27]. In the present study, we extended the previous findings by demonstrating that compared with other members of the atypical MAPK family, MAPK4 was highly expressed in ECs of NSCLC, and its expression was related to increased tumor vascular density. Notably, we found that targeted silencing of MAPK4 in ECs also inhibited angiogenesis and abrogated the tumorigenesis of NSCLC in vivo. Moreover, we analyzed clinical samples of patients with NSCLC and found that the expression of MAPK4 was higher in tumor tissues than that in adjacent tissues. CD34 is a representative marker of new vessels. Our results showed that the expression of MAPK4 in cells expressing CD34 was closely related to the poor prognosis of patients with NSCLC. Therefore, our data revealed a novel biological role for MAPK4 in angiogenesis during NSCLC tumorigenesis, which suggests a pivotal role for MAPK4 in the development of NSCLC.

ECs play a key role in neovascularization during angiogenesis. Many studies have reported that MAPKs
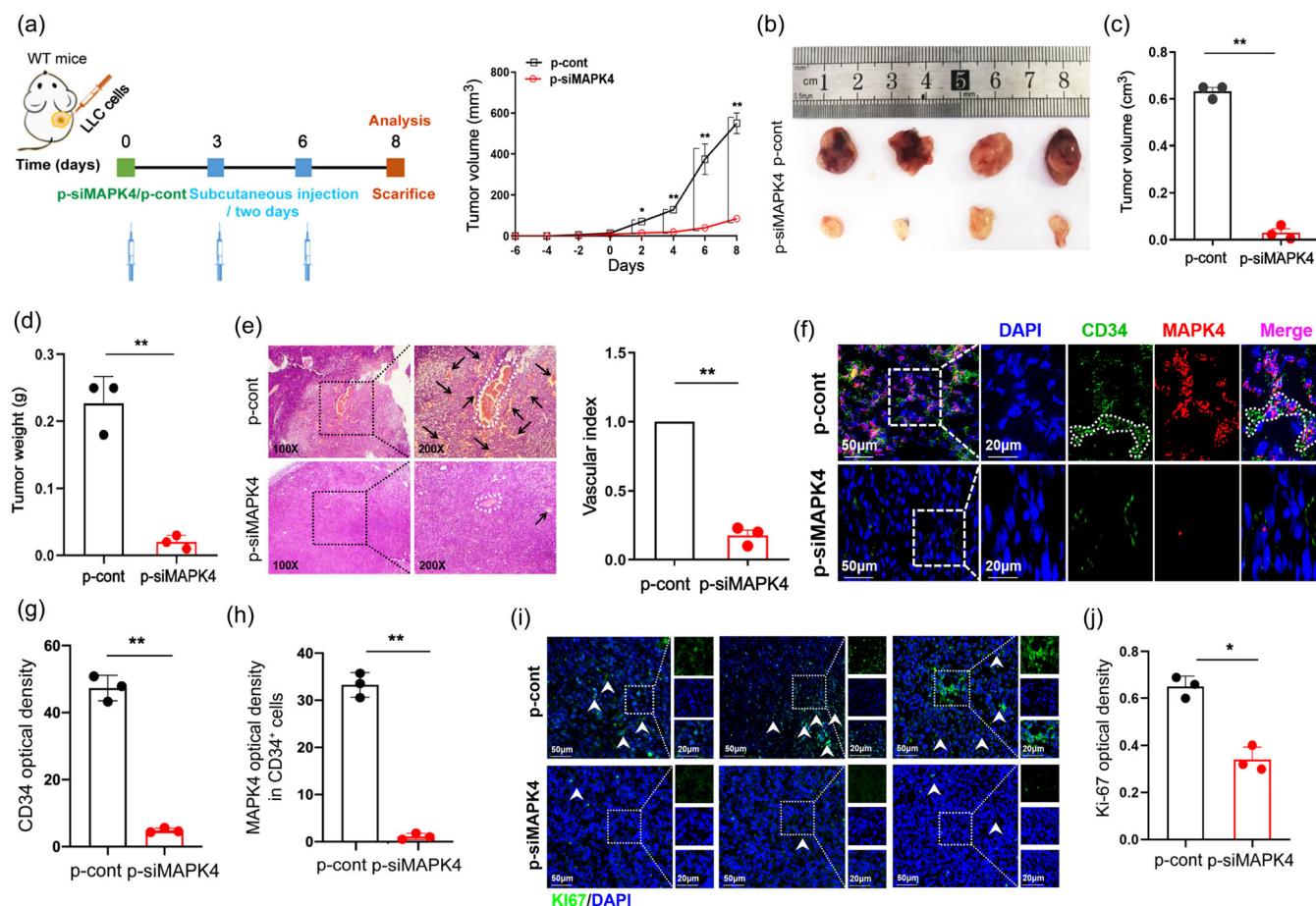
FIGURE 6 Targeted intervention of the expression of mitogen-activated protein kinase 4 (MAPK4) could inhibit the growth of non-small cell lung cancer (NSCLC) tumor in vivo. Lewis lung carcinoma (LLC) cells (5×10^5) were subcutaneously injected into the right flanks of wild-type (WT) C57BL/6 mice. Tumors were collected on day 21. (a) Schematic diagram showing subcutaneously injection of LLC cells (5×10^5) into the right flanks of WT mice. Seven days later, the constructed PGL3.0 basic-CD34 promoter-MAPK4 RNA interference (RNAi) eukaryotic expression vectors (termed as p-siMAPK4) or p-cont given by subcutaneous injection into the left flank of murine NSCLC tumor model three times every 3 days. Tumor growth was monitored every 2 days to generate the growth curve, and tumors were collected on day 14. (b) Tumor size. (c) Tumor volume and (d) tumor weight. (e) Tumor pathology was analyzed by hematoxylin-eosin (H&E) staining. The arrows indicate neovascularization. (f–h) The expression of MAPK4 and CD34 in tumors was analyzed by immunofluorescence and quantitated. (i, j) Cell proliferation nuclear antigen (Ki67) expression in tumors was analyzed by immunofluorescence and quantitated. Representative data from three independent experiments were shown. *$p < 0.05$, **$p < 0.01$.

are involved in the proliferation and growth of ECs under different conditions. For example, Li et al. [33] found that elevated p38 and ERK1/2 activity was associated with apoptosis of ECs. Wang et al. [34] reported that the low levels of H_2O_2 significantly promoted the proliferation, migration, and tube formation of ECs through the JNK pathway. Our results herein showed that MAPK4 silencing impaired the proliferation, colony-forming and tube-forming abilities of HUVECs in vitro, accompanied by cell cycle arrest and altered expression of cell cycle-related genes.

To reproduce the tumor microenvironment in vitro, we cultured HUVECs in the supernatant of human NSCLC cells. Under these conditions, MAPK4 silencing also inhibited the growth of HUVECs in vitro, which was consistent with the experimental results in vivo. In line with these findings, global gene expression analysis showed that MAPK4 silencing resulted in changes in the expression patterns of cell cycle-related genes. The mechanism by which MAPK4 silencing induces S-phase arrest in HUVECs requires further study. Additionally, we found that MAPK4 silencing did not affect the migration ability of ECs. These results indicated that MAPK4 plays an important role in the growth of ECs, thereby promoting the angiogenesis of NSCLC. Recent studies have shown that interactions among multiple cells in the tumor microenvironment, including tumor cells, ECs, and immune cells, are important for tumor
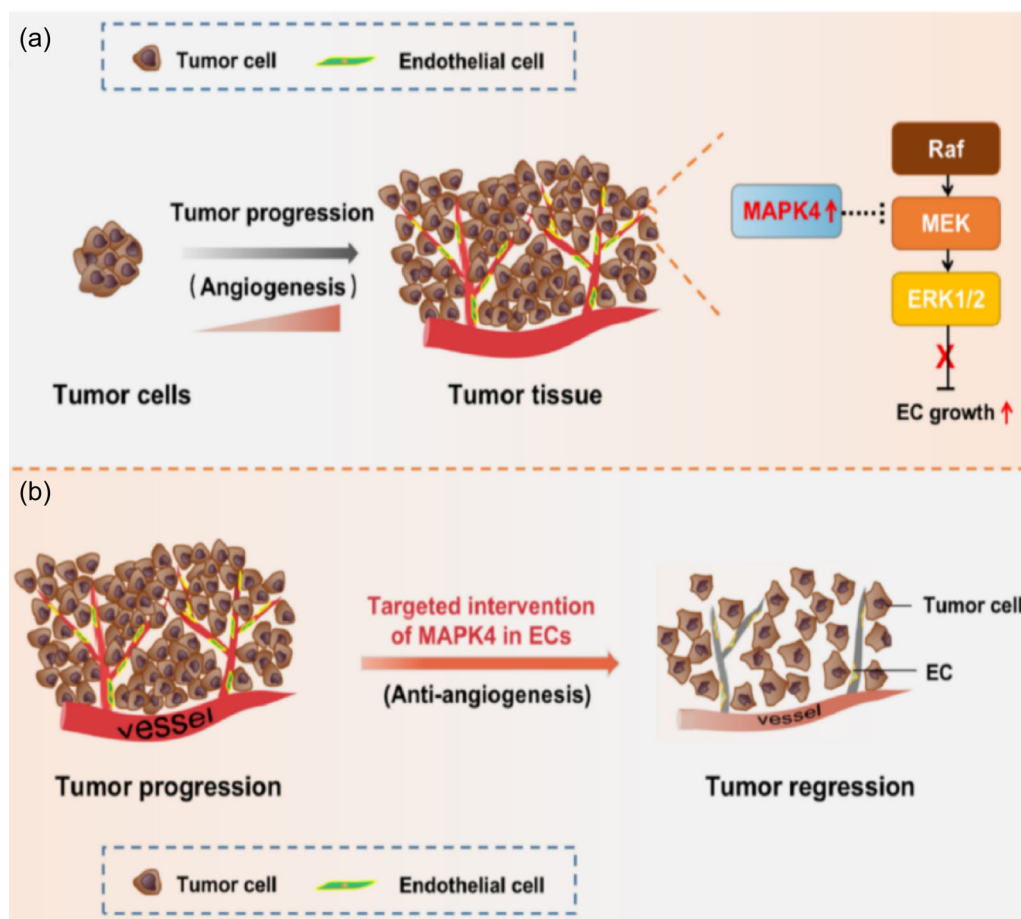
FIGURE 7 Schematic diagram of mitogen-activated protein kinase 4 (MAPK4) role in tumor angiogenesis and progression of non-small cell lung cancer (NSCLC). (a) MAPK4 facilitates tumor angiogenesis and progression in NSCLC by promoting the growth of endothelial cell (CD34$^+$ EC), which is related to altered transduction of Raf/MEK/ERK1/2 signaling pathway. (b) Targeted intervention the expression of MAPK4 in CD34$^+$ ECs can repress tumor angiogenesis and progression of NSCLC. ERK1/2, extracellular regulated protein kinases 1/2; MEK, mitogen-activated extracellular signal-regulated kinase; Raf, rapidly accelerated fibrosarcoma.

angiogenesis. Therefore, it may be valuable to further explore the potential influence of other cells in local tumor tissues on the expression of MAPK4 in ECs. This information may help aid in the identification of the exact biological function of MAPK4 in tumor angiogenesis and development of NSCLC.

Multiple signaling pathways, such as the MAPK, AKT, and NF-κB pathways, are connected by complex networks in eukaryotic cells, including ECs, and control gene expression, cell survival, apoptosis, and cell differentiation [35–38]. Notably, our results showed that MAPK4 silencing did not affect the AKT, JNK, and NF-κB signaling pathways in ECs. However, signal transduction through the Raf/MEK/ERK1/2 pathway was significantly increased in the absence of MAPK4 and in HUVECs cultured in the supernatant of human NSCLC cells. Importantly, inhibition of ERK1/2 pathway reversed the effect of MAPK4 silencing on the growth and tube-forming ability of ECs. The ERK1/2 pathway plays

an important role in the growth of ECs. For example, Zong et al. [39] reported that Notch1 protects against cigarette smoke-induced endothelial apoptosis in chronic obstructive pulmonary disease by inhibiting the ERK pathway. Taken together, these data indicated that the effect of MAPK4 silencing on the proliferation of HUVECs is related to the altered signal transduction through the Raf/MEK/ERK1/2 signaling pathway. Notably, Chen et al. [40] reported that administration of liraglutide promoted the activation of ERK and the survival of ECs, indicating that the ERK1/2 pathway also might play distinct roles in the growth of ECs under different conditions. Moreover, in our previous study, we found that MAPK4 deficiency altered signal transduction through the NF-κB and JNK pathways in ALI [18]. We speculate that the results of these studies reflect the complexity of the exact roles of the networks connecting these pathways in different experimental settings. Thus, the precise interaction between MAPK4 and the

Raf/MEK/ERK1/2 pathway in the tumor angiogenesis and development of NSCLC needs to be fully elucidated.

5 | CONCLUSION

Our study revealed a previously unknown role for the atypical MAPK member MAPK4 in the angiogenesis and development of NSCLC. Our findings indicate that MAPK4 regulates the growth of ECs and accelerates angiogenesis through the ERK1/2 pathway, thus promoting the progression of NSCLC (Figure 7a). Furthermore, targeted intervention of MAPK4 expression in ECs might be a valuable clinical strategy to inhibit angiogenesis and induce tumor regression (Figure 7b). These findings indicate that MAPK4 may be a new clinical therapeutic target for NSCLC.

AUTHOR CONTRIBUTIONS
Jing Chen, Jing Yang, and Yufang Liu designed the research. Jing Chen, Jing Yang, Yufang Liu, Juanjuan Zhao, Lin Tang, Xu Zhao, and Zhenke Wen conducted experiments. Jing Chen, Jing Yang, Yufang Liu, Ya Zhou, Chao Chen, Dongmei Li, and Mengmeng Guo analyzed data. Jing Chen, Jing Yang, and Yufang Liu wrote and revised this manuscript. Lin Xu and Guiyou Liang revised the manuscript and supervised the research. All authors read and approved the final manuscript.

ACKNOWLEDGMENTS
We thank AJE (www.aje.cn.com) for linguistic assistance and scientific consultation during the preparation of this manuscript.

CONFLICT OF INTEREST STATEMENT
The authors declare no conflict of interest.

DATA AVAILABILITY STATEMENT
The data sets in this study are available from the corresponding author on reasonable request.

ETHICS STATEMENT
Animal experiments were approved by and followed the ethical guidelines of the Zunyi Medical University Laboratory Animal Care and Use Committee, China (No. 2018016). The data extraction and tissue microarray construction of patients with lung cancer were approved by the ethics committee of Shanghai Outdo Biotech Co., Ltd. All authors of this study have seen and approved the current version of the manuscript.

INFORMED CONSENT
The authors have nothing to report.

ORCID
Lin Xu http://orcid.org/0000-0002-6889-0279

REFERENCES
1. Ettinger DS, Akerley W, Borghaei H, Chang AC, Cheney RT, Chirieac LR, et al. Non-small cell lung cancer, version 2.2013. J Natl Comp Cancer Netw. 2013;11(6):645–53. https://doi.org/10.6004/jnccn.2013.0084
2. Huang Y, Zhang L. Annual progress of clinical research on targeted therapy for nonsmall cell lung cancer in 2022. Cancer Innov. 2023;2(1):25–35. https://doi.org/10.1002/cai2.56
3. Xu Z, Zou Z, Hao X, Xing P, Li J. Adjuvant and neo-adjuvant immunotherapy in resectable non-small cell lung cancer (NSCLC): current status and perspectives. Cancer Innov. 2023;2(1):65–78. https://doi.org/10.1002/cai2.49
4. Passiglia F, Bertaglia V, Reale ML, Delcuratolo MD, Tabbò F, Olmetto E, et al. Major breakthroughs in lung cancer adjuvant treatment: looking beyond the horizon. Cancer Treat Rev. 2021;101:102308. https://doi.org/10.1016/j.ctrv.2021.102308
5. Fox SB, Gatter KC, Harris AL. Tumour angiogenesis. J Pathol. 1996;179(3):232–7. https://doi.org/10.1002/(SICI)1096-9896(199607)179
6. Holash J, Maisonpierre PC, Compton D, Boland P, Alexander CR, Zagzag D, et al. Vessel cooption, regression, and growth in tumors mediated by angiopoietins and VEGF. Science. 1999;284(5422):1994–8. https://doi.org/10.1126/science.284.5422.1994
7. Zhang K, Yang L, Wang J, Sun T, Guo Y, Nelson R, et al. Ubiquitin-specific protease 22 is critical to in vivo angiogenesis, growth and metastasis of non-small cell lung cancer. Cell Commun Signal. 2019;17(1):167. https://doi.org/10.1186/s12964-019-0480-x
8. Zhuo H, Zhao Y, Cheng X, Xu M, Wang L, Lin L, et al. Tumor endothelial cell-derived cadherin-2 promotes angiogenesis and has prognostic significance for lung adenocarcinoma. Mol Cancer. 2019;18(1):34. https://doi.org/10.1186/s12943-019-0987-1
9. Handy Jr., JR. Minimally invasive lung surgery and post-operative quality of life. Thorac Surg Clin. 2012;22(4):487–95. https://doi.org/10.1016/j.thorsurg.2012.07.010
10. Mao Z, Xu B, He L, Zhang G. PVT1 promotes angiogenesis by regulating miR-29c/vascular endothelial growth factor (VEGF) signaling pathway in non-small-cell lung cancer (NSCLC). Med Sci Monit. 2019;25:5418–25. https://doi.org/10.12659/MSM.917601
11. Garcia J, Hurwitz HI, Sandler AB, Miles D, Coleman RL, Deurloo R, et al. Bevacizumab (Avastin®) in cancer treatment: a review of 15 years of clinical experience and future outlook. Cancer Treat Rev. 2020;86:102017. https://doi.org/10.1016/j.ctrv.2020.102017
12. Alshangiti A, Chandhoke G, Ellis PM. Antiangiogenic therapies in non-small-cell lung cancer. Curr Oncol. 2018;25(Suppl 1):45–58. https://doi.org/10.3747/co.25.3747
13. Zhao J, Guo M, Yan Y, Wang Y, Zhao X, Yang J, et al. The miR-7/EGFR axis controlsthe epithelial cell immunomodulation and regeneration and orchestrates the pathology in inflammatory bowel disease. J Adv Res. 2023;57:119–34. https://doi.org/10.1016/j.jare.2023.04.011
14. Liu Y, Yang H, Xiong J, Zhao J, Guo M, Chen J, et al. Icariin as an emerging candidate drug for anticancer treatment: current

status and perspective. Biomed Pharmacother. 2023;157: 113991. https://doi.org/10.1016/j.biopha.2022.113991

15. Altorki NK, Markowitz GJ, Gao D, Port JL, Saxena A, Stiles B, et al. The lung microenvironment: an important regulator of tumour growth and metastasis. Nat Rev Cancer. 2019;19(1): 9–31. https://doi.org/10.1038/s41568-018-0081-9

16. Ge G, Wang A, Yang J, Chen Y, Yang J, Li Y, et al. Interleukin-37 suppresses tumor growth through inhibition of angiogenesis in non-small cell lung cancer. J Exp Clin Cancer Res. 2016;35:13. https://doi.org/10.1186/s13046-016-0293-3

17. Pearson G, Robinson F, Beers Gibson T, Xu B, Karandikar M, Berman K, et al. Mitogen-activated protein (MAP) kinase pathways: regulation and physiological functions. Endocr Rev. 2001;22(2):153–83. https://doi.org/10.1210/edrv.22.2.0428

18. Mao L, Zhou Y, Chen L, Hu L, Liu S, Zheng W, et al. Identification of atypical mitogen-activated protein kinase MAPK4 as a novel regulator in acute lung injury. Cell Biosci. 2020;10:121. https://doi.org/10.1186/s13578-020-00484-2

19. Zhao J, Chu F, Xu H, Guo M, Shan S, Zheng W, et al. C/EBPα/miR-7 controls CD4+ T-cell activation and function and orchestrates experimental autoimmune hepatitis in mice. Hepatology. 2021;74(1):379–96. https://doi.org/10.1002/hep.31607

20. Wu YS, Chen YT, Bao YT, Li ZM, Zhou XJ, He JN, et al. Identification and verification of potential therapeutic target genes in berberine-treated zucker diabetic fatty rats through bioinformatics analysis. PLoS One. 2016;11(11):e0166378. https://doi.org/10.1371/journal.pone.0166378

21. Berriri S, Garcia AV, dit Frey NF, Rozhon W, Pateyron S, Leonhardt N, et al. Constitutively active mitogen-activated protein kinase versions reveal functions of *Arabidopsis* MPK4 in pathogen defense signaling. Plant Cell. 2012;24(10): 4281–93. https://doi.org/10.1105/tpc.112.101253

22. El-Aarag SA, Mahmoud A, Hashem MH, Elkader HA, Hemeida AE, ElHefnawi M. In silico identification of potential key regulatory factors in smoking-induced lung cancer. BMC Med Genomics. 2017;10(1):40. https://doi.org/10.1186/s12920-017-0284-z

23. Tian S, Lou L, Tian M, Lu G, Tian J, Chen X. MAPK4 deletion enhances radiation effects and triggers synergistic lethality with simultaneous PARP1 inhibition in cervical cancer. J Exp Clin Cancer Res. 2020;39(1):143. https://doi.org/10.1186/s13046-020-01644-5

24. Du SY, Huang XX, Li NM, Lv CY, Lv CH, Wei ML, et al. MiR-127-3p inhibits proliferation of ovarian cancer in rats through down-regulating MAPK4. Eur Rev Med Pharmacol Sci. 2020;24(20):10383–90. https://doi.org/10.26355/eurrev_202010_23388

25. Guo LH, Li H, Wang F, Yu J, He JS. The tumor suppressor roles of miR-433 and miR-127 in gastric cancer. Int J Mol Sci. 2013;14(7):14171–84. https://doi.org/10.3390/ijms140714171

26. Wang W, Han D, Cai Q, Shen T, Dong B, Lewis MT, et al. MAPK4 promotes triple negative breast cancer growth and reduces tumor sensitivity to PI3K blockade. Nat Commun. 2022;13(1):245. https://doi.org/10.1038/s41467-021-27921-1

27. Wang W, Shen T, Dong B, Creighton CJ, Meng Y, Zhou W, et al. MAPK4 overexpression promotes tumor progression via noncanonical activation of AKT/mTOR signaling. J Clin Invest. 2019;129(3):1015–29. https://doi.org/10.1172/JCI97712

28. Coulombe P, Meloche S. Atypical mitogen-activated protein kinases: structure, regulation and functions. Biochim Biophys Acta Mol Cell Res. 2007;1773(8):1376–87. https://doi.org/10.1016/j.bbamcr.2006.11.001

29. Kaminska B, Gozdz A, Zawadzka M, Ellert-Miklaszewska A, Lipko M. MAPK signal transduction underlying brain inflammation and gliosis as therapeutic target. Anat Rec. 2009;292(12):1902–13. https://doi.org/10.1002/ar.21047

30. Shen T, Wang W, Zhou W, Coleman I, Cai Q, Dong B, et al. MAPK4 promotes prostate cancer by concerted activation of androgen receptor and AKT. J Clin Invest. 2021;131(4): e135465. https://doi.org/10.1172/JCI135465

31. Lu L, Liu Q, Wang P, Wu Y, Liu X, Weng C, et al. MicroRNA-148b regulates tumor growth of non-small cell lung cancer through targeting MAPK/JNK pathway. BMC Cancer. 2019;19(1):209. https://doi.org/10.1186/s12885-019-5400-3

32. Zhang X, Han S, Zhou H, Cai L, Li J, Liu N, et al. TIMM50 promotes tumor progression via ERK signaling and predicts poor prognosis of non-small cell lung cancer patients. Mol Carcinog. 2019;58(5):767–76. https://doi.org/10.1002/mc.22969

33. Li S, Zhong M, Yuan Y, Zhang L. Differential roles of p38 MAPK and ERK1/2 in angiopoietin-2-mediated rat pulmonary microvascular endothelial cell apoptosis induced by lipopolysaccharide. Exp Ther Med. 2018;16(6):4729–36. https://doi.org/10.3892/etm.2018.6810

34. Wang Z, Yang J, Qi J, Jin Y, Tong L. Activation of NADPH/ROS pathway contributes to angiogenesis through JNK signaling in brain endothelial cells. Microvasc Res. 2020;131:104012. https://doi.org/10.1016/j.mvr.2020.104012

35. Soares-Silva M, Diniz FF, Gomes GN, Bahia D. The mitogen-activated protein kinase (MAPK) pathway: role in immune evasion by trypanosomatids. Front Microbiol. 2016;7:183. https://doi.org/10.3389/fmicb.2016.00183

36. Droguett D, Carrillo I, Castillo C, Gómez F, Negrete M, Liempi A, et al. Trypanosoma cruzi induces cellular proliferation in the trophoblastic cell line BeWo. Exp Parasitol. 2017;173:9–17. https://doi.org/10.1016/j.exppara.2016.12.005

37. dos-Santos GRRM, Fontenele MR, Dias FA, Oliveira PL, Nepomuceno-Silva JL, de Melo LDB, et al. Functional studies of TcRjl, a novel GTPase of trypanosoma cruzi, reveals phenotypes related with MAPK activation during parasite differentiation and after heterologous expression in *Drosophila* model system. Biochem Biophys Res Commun. 2015;467(1):115–20. https://doi.org/10.1016/j.bbrc.2015.09.110

38. Zhang C, Wang J, Lü G, Li J, Lu X, Mantion G, et al. Hepatocyte proliferation/growth arrest balance in the liver of mice during E. multilocularis infection: A coordinated 3-stage course. PLoS One. 2012;7(1):e30127. https://doi.org/10.1371/journal.pone.0030127

39. Zong D, Li J, Cai S, He S, Liu Q, Jiang J, et al. Notch1 regulates endothelial apoptosis via the ERK pathway in chronic obstructive pulmonary disease. Am J Physiol Cell Physiol. 2018;315(3): C330–40. https://doi.org/10.1152/ajpcell.00182.2017

40. Chen Y, Liu C, Zhou P, Li J, Zhao X, Wang Y, et al. Liraglutide reduces coronary endothelial cells no-reflow damage through activating MAPK/ERK signaling pathway. J Recept Signal

Transduct. 2021;41(6):553–7. https://doi.org/10.1080/10799893.2020.1833921

SUPPORTING INFORMATION

Additional supporting information can be found online in the Supporting Information section at the end of this article.